HHS Public Access

Author manuscript

Liver Int. Author manuscript; available in PMC 2016 April 01.

Published in final edited form as:

Liver Int. 2015 April ; 35(4): 1213–1221. doi:10.1111/liv.12606.

Integrin-Linked Kinase Regulates Endothelial Cell Nitric-oxide Synthase Expression in Hepatic Sinusoidal Endothelial Cells

Mahnoush S. Shafiei[1], **Songling Lui**[2], and **Don C. Rockey**[2]

[1]Division of Digestive and Liver Diseases, University of Texas Southwestern Medical Center, Dallas, TX

[2]The Department of Medicine, The Medical University of South Carolina, Charleston, SC

Abstract

Background—Portal hypertension results from endothelial dysfunction after liver injury caused in part by abnormal production of endothelial cell derived nitric oxide synthase (eNOS). Here, we have postulated that endothelial mechanosensing pathways involving integrin linked kinase (ILK) may play a critical role in portal hypertension, eNOS expression and function.

Aims—In this study, we investigated the role of ILK and the small GTP-binding protein, Rho, in sinusoidal endothelial cell eNOS regulation and function.

Methods—Primary liver sinusoidal endothelial cells (SECs) were isolated using standard techniques. Liver injury was induced by performing bile duct ligation (BDL). To examine the expression of Rho and ILK *in vivo* during wound healing, SECs were infected with constitutively active Rho (V14), a dominant negative Rho (N19) and constructs encoding ILK and a short hairpin-inhibiting ILK.

Results—ILK expression was increased in SECs after liver injury; endothelin-1, vascular endothelial growth factor, and transforming growth factor beta-1 stimulated ILK expression in SECs. ILK expression in turn led to eNOS upregulation and to enhanced eNOS phosphorylation and NO production. ILK knockdown or ILK (kinase) inhibition reduced eNOS mRNA expression, promoter activity, eNOS expression, and ultimately NO production. In contrast, ILK over-expression had the opposite effect. Inhibition of ILK activity also disrupted the actin cytoskeleton in isolated SECs. Rho overexpression suppressed phosphorylation of the serinethreonine kinase, Akt, and inhibited eNOS phosphorylation. Finally, inhibition of Rho function with the RGS domain of the p115-Rho-specific GEF (p115-RGS) significantly increased eNOS phosphorylation.

Conclusions—Our data suggest a potential role for ILK, the cytoskeleton, and ILK signaling partners including Rho in regulating intrahepatic SEC eNOS expression and function.

Keywords

liver; cirrhosis; portal hypertension; signaling; rho; rho kinase

Correspondence: Don C. Rockey, M.D. Department of Internal Medicine Medical University of South Carolina 96 Jonathan Lucas Street, Suite 803 Charleston, SC 29425 rockey@musc.edu Telephone: 843-792-2914 Fax: 843-792-5265.

Disclosures: The authors have no financial relationships relevant to this study.

Introduction

The endothelium plays a critical role in modulation of vascular tone (1, 2). Endothelial dysfunction occurring after injury is classically associated with abnormalities in endothelium-dependent relaxation of blood vessels in response to the endogenous vasodilator nitric oxide (NO) (3). Endothelial dysfunction is concomitant with changes in vascular structure associated with many forms of vascular disease, such as hypertension and atherosclerosis. Likewise, portal hypertension, occurring after essentially all forms of liver injury, appears to be an endothelialopathy, associated with abnormal production of endothelial cell derived eNOS (3-5). The mechanism for this defect appears to be linked to abnormal phosphorylation of eNOS (5-7); indeed, after liver injury, a multitude of signaling events contribute to a reduction in eNOS phosphorylation (3, 5, 8). For example, Akt phosphorylation is abnormal, and this contributes to reduced eNOS activity and NO synthesis in injured endothelial cells (3, 5).

The Rho GTPases are members of the Ras superfamily of small GTP-binding proteins and major substrates for posttranslational modification (9). Activators of Rho include growth factors, cytokines, integrins, and G protein– coupled receptor ligands or hormone (10). RhoA negatively regulates the production of endothelium-derived nitric oxide via Rho-induced changes in the endothelial actin cytoskeleton (11). Indeed, direct inhibition of Rho by Y-27632 or disruption of the endothelial actin cytoskeleton by cytochalasin D leads to increases in aortic eNOS expression and activity in mice (12).

Integrin-linked kinase (ILK), a key regulator of blood vessel integrity, is a PI3-kinase-dependent serine/threonine protein kinase that interacts with the cytoplasmic domains of both β1 and β3 integrins and lies upstream of many intracellular signaling pathways (13). ILK plays essential roles in endothelial and extracellular matrix – mediated signaling, matrix-endothelial cell interactions, cell survival, and the recruitment of endothelial progenitors (14). Given that integrin signaling depends on the effects of RhoA on the actin cytoskeleton, and that ILK is likewise important in activation of RhoA and that Rho may be involved in eNOS signaling, we have hypothesized here that ILK and Rho play a role in the regulation of eNOS and perhaps its activity in sinusoidal endothelial cells.

Experimental procedures

Materials

Endothelin-1 (ET-1) and BQ-788 (endothelin-B receptor antagonist) were from American Peptide Co. Inc. (Sunnyvale, CA). Recombinant VEGF, EGF and TGF-β were from R&D Systems (Minneapolis, MN). Mouse anti-ILK monoclonal antibody, anti-eNOS and -phospho-eNOS (Ser-1179) antibodies were from BD Transduction Laboratories (Lexington, KY). Polyclonal anti-total-Akt, anti-phospho-Akt (Ser-473) antibodies were from Cell Signaling Technologies (Beverly, MA). Anti-rabbit IgG/horseradish peroxidase conjugate or anti-mouse IgG/horseradish peroxidase conjugate were from Promega (Madison, WI).

Cell Isolation and Culture

Sinusoidal endothelial cells were isolated from male Sprague-Dawley rats (450–500 g) (Harlan, Indianapolis, IN). In brief, after *in situ* perfusion of the liver with 20 mg % Pronase (Roche Molecular Biochemicals, Indianapolis, IN), followed by collagenase (Worthington Biochemical Corporation, Lakewood, NJ), dispersed cell suspensions were removed from a layered discontinuous density gradient of 8.2 and 15.6% Accudenz (Accurate Chemical and Scientific, Westbury, NY), further purified by centrifugal elutriation (18 ml/min flow), and grown in medium containing 20% serum (10% horse/calf). The purity of endothelial cells was documented by their uptake of fluorescently labeled di-I-acetoacetylated low-density lipoprotein. Only primary sinusoidal endothelial isolates of at least 95% purity were used for study.

Animal Models of Liver Injury

Liver injury was induced by the administration of carbon tetrachloride (CCl_4) or by performing bile duct ligation (BDL) as described previously (15). BDL resulted in periportal expansion of the biliary duct cells with concomitant periductular and lobular extracellular matrix deposition. In sham-operated rats, an incision was made in the abdomen, which was then closed without any treatment. Carbon tetrachloride administration led to central and central-portal extracellular matrix deposition. Animal protocols used to induce injury and fibrogenesis were approved by the University of Texas Southwestern Medical Center Animal Care and Use Guidelines Committee.

Nitric Oxide Measurement

In order to evaluate NO production, we analyzed the release of nitrite, the stable breakdown product of NO, by using a Sievers Chemiluminescence NO Analyzer (Sievers Instruments, Inc., Boulder, CO) as descried previously (16).

Immunoblotting

Cell lysates were prepared in a buffer containing 1% Triton X-100, 150mM NaCl, 20mM Tris, pH 7.5, 1mM EDTA, 50mM NaF, 50mM sodium-2-glycerophosphate, 0.05mM Na3VO4, 10mg/ml leupeptin, 10% glycerol, and 100mM phenylmethylsulfonyl fluoride. Samples containing 50μg of total protein were subjected to SDS–PAGE, after which proteins were transferred to nitrocellulose membranes (Schleicher & Schuell, Keene, NH). Membranes were incubated for 1 h at room temperature in blocking buffer (10 mM sodium phosphate, 0.5MNaCl, 0.05% Tween 20, and 2.5% dry milk) and then with primary antibody (1:1000) overnight at 4 °C. Membranes were then washed of excess primary antibody at room temperature in a phosphate-buffered saline Tween buffer (TBST: 10mM 0.05%, Tris pH 8, 0.9% sodium chloride, Tween 20 0.05%) and incubated for 1 h at room temperature with secondary antibody. After washing, specific signals were visualized using enhanced chemiluminescence detection pursuant to the manufacturer's instructions (Pierce). Specific bands were scanned and data collected over a narrow range of X-ray film (Eastman Kodak, Rochester, NY) linearity and quantitated by scanning densitometry.

Real-Time PCR

Total RNA was extracted with Trizol reagent according to the manufacturer's instructions (Invitrogen, Carlsbad, CA). One microgram of RNA was reverse-transcribed using an oligo (dt) primer and Superscript RNase H-reverse transcriptase as per the manufacturer's directions (Invitrogen). Amplification reactions were performed using SYBR Green PCR Master Mix (Applied Biosystems, Foster City, CA). Primer sequences were as follows: GAPDH forward, 5′-ATTGAC CAC TAC CTG GGC AA-3′; and reverse, 5′-GAG ATACAC TTC AAC ACT TTG ACCT-3′; eNOS forward, 5′-CTGTGGTCTGGTGCTGGTC-3′; reverse5′-TGGGCAACTTGAAGAGTGTG-3′; were synthesized by Integrated DNA Technologies. In all, 5 μl of diluted cDNA samples (1:5 dilution) were used in a quantitative two-step PCR (a 10-min step at 95 °C followed by 50 cycles of 15 s of 95 °C and 1 s at 65 °C) in the presence of 400nM specific forward and reverse primers, and SYBR Green PCR Master Mix. Each sample was analyzed in triplicate using an ABI system (7900HT Fast Real-Time PCR). As negative controls, water was used as a template for each reaction.

Adenoviral Gene Transfer

Endothelial cells were infected with constitutively active Rho (V14), a dominant negative Rho (N19); each kindly provided by Dr. Aviv Hassid, University of Tennessee), p115-RGS (a gift of Dr. Patrick Casey, Duke University Medical Center), or a matched adenovirus containing GFP as a control, at MOI of 100. Adenoviral constructs encoding ILK and a short hairpin-inhibiting ILK were prepared as previously described (17). The infection efficiency of the adenovirus was monitored by the expression of GFP and typically reached 80–90% within 48 h. Viral titers were measured by standard plaque assay using 293 cells. For *in vivo* animal experiments, adenovirus was injected into the inferior vena cava at the time of BDL surgery in 500 L of PBS at a concentration of 1×10^{10} pfu/Kg.

Luciferase assay

Cells were plated in 6-well plates and grown to 70% confluence. At that time, transfection was performed with Lipofectin Reagent (Life Technologies) using a protocol recommended by the manufacturer. The cells were then cotransfected with 1.2 μg of eNOS promoter linked to a firefly luciferase reporter gene (eNOS-Luc) and 0.5 ng of promoter-renilla luciferase (pRL) reporter control plasmid per well for 48 h according to the manufacturer's protocol (Promega, Madison, WI). Transfections were performed in triplicates, and the experiments were repeated three times.

Morphometry

Livers were fixed in 10% phosphate-buffered formalin for 48 h at 4 °C, washed twice with water, stored in 70% ethanol at 4 °C for 24 h, and then embedded in paraffin. Five-micron sections were then dehydrated and stained with 0.1% sirius red in saturated picric acid and counterstained with fast green (all from Sigma).

Immunofluorescence

Cells were cultured as above for 36 hours and exposed to QLT0267 (25μM) for 48 hours. They were then washed, permeabilized and fixed with 3% paraformaldehyde and 0.5%. Triton X-100 in PBS for 10 min followed by labeling with Texas Red-phalloidin (Molecular Probes) and Dapi (Alexis, San Diego, CA) to identify nuclei. After washing and mounting, signals were visualized with a Zeiss LSM 510 META confocal microscope.

Statistical Analysis

Data are expressed as means ± S.E.M. Statistical analysis was performed by using an independent Student's t-test or one-way analysis of variance with the Tukey *post hoc* test when appropriate. A *P*-value <0.05 was considered to be statistically significant.

Results

Up-regulation of ILK expression in sinusoidal endothelial cells after injury

To examine the expression of ILK in sinusoidal endothelial cells *in vivo* during wound healing, liver injury created by bile duct ligation, or after exposure of rats to repetitive doses of CCl4, sinusoidal endothelial cells were subsequently isolated and immediately subjected immunoblotting to detect ILK. Regardless of the type of liver injury, ILK expression was significantly up-regulated in sinusoidal endothelial cells (**Figure 1A & 1B**).

ILK modifies the wound-healing response to injury in vivo

We administered adenoviral constructs containing GFP, shILK or ILK to control or injured (BDL) rats (**Figure 1C-G**) and assessed typical wound-healing phenotypes. We found that inhibition of ILK with the shILK construct led to reduced fibrogenesis (**Figure 1E**), while overexpression of ILK during the wounding response led to markedly enhanced fibrogenesis (**Figure 1F**).

ILK expression is regulated by elements found in the wound-healing environment

The liver injury response is characterized by production of cytokines and a variety of peptides that help drive the wounding response. Therefore, we examined typical compounds found in the wounding environment, including EGF, ET-1, VEGF and TGF-β. After stimulation of sinusoidal endothelial cells with these factors, we found that ET-1, VEGF and TGF-β, all had potent stimulating effects, while EGF did not stimulate ILK expression (**Figure 1H**). We also demonstrated a dose-response relationship between ET-1 concentration and stimulation of ILK expression (**Figure 2A**) and that the stimulation of ILK by ET-1 appeared to occur at least partially via ET_B receptors, the latter of which are found on sinusoidal endothelial cells (Figure 2B).

The effect of ILK on eNOS expression and function

We next demonstrated that we were able to manipulate ILK expression using specific constructs to overexpress (an adenovirus expressing ILK, Ad-ILK) or reduce (an adenovirus expressing ILK small interfering short hairpin RNA AdshILK) ILK in isolated sinusoidal endothelial cells (**Figure 2C**). Adenovirus expressing GFP (Ad-GFP) was used as a control.

When ILK was overexpressed in sinusoidal endothelial cells exposed to ET-1, eNOS and eNOS phosphorylation were markedly increased compared to control (**Figure 3A**); eNOS phosphorylation closely paralleled the expression of total eNOS (**Figure 3A).** In contrast, ILK inhibition abrogated this effect. Additionally, NO synthesis paralleled the effect on total eNOS (**Figure 3B**).

In order to determine the effects of ILK inhibition on the cytoskeleton of SEC's, we exposed sinusoidal endothelial cells to QLT-0267, a specific ILK kinase inhibitor. Exposure of SEC's to QLT-0267 led to disruption of actin filaments (**Figure 4).**

We next examined the role of ILK in modulating eNOS phosphorylation (**Figure 5A**). Inhibition of ILK (kinase) activity with QLT0267 inhibited both eNOS expression and eNOS phosphorylation (serine 1179) and reduced nitrite synthesis (**Figure 5B**). Further, exposure of sinusoidal endothelial cells to QLT-0267 reduced eNOS promoter activity (**Figure 5C**). Overexpression of ILK with adenovirus increased eNOS transcriptional activity, while inhibition of ILK expression reduced eNOS transcription (**Figure 5D**).

Effect of Rho on Akt activity and eNOS gene expression

We and others have previously demonstrated that Akt mediates eNOS phosphorylation, and subsequent NO synthesis (16, 18). We have also shown that Rho plays an important role ILKs effect on the actin cytoskeleton and mediating changes in cell shape (19). Therefore, to further investigate the role of Rho in eNOS function, we examined the effect of manipulation of Rho on AKT phosphorylation, and eNOS expression and phosphorylation. Activation of Rho with a recombinant adenovirus expressing constitutive active Rho (Rho V14) led to reduced Akt activation, while a dominant negative Rho inhibited Akt phosphorylation (**Figure 6 A/B**). Next, we investigated Rho's effect on eNOS expression. Sinusoidal endothelial cells infected with recombinant adenovirus expressing active RhoV14 and shILK decreased eNOS expression and its phosphorylation whereas dominant negative Rho (Rho N19) or Ad-ILK significantly increased eNOS expression (**Figure 6C**) and phosphorylation (**Figure 6D**).

To further investigate the role of Rho in the regulation of eNOS, sinusoidal endothelial cells were infected with an adenovirus containing the RGS domain of p115RhoGEF. Inhibition of Rho-GTPase with this construct had minimal effect on eNOS and caused a significant increase in eNOS phosphorylation (**Figure 7**), suggesting that the Rho-GTPase pathways play an important role in both eNOS expression, but also its phosphorylation and activation.

Discussion

Here, we have demonstrated that ILK regulates eNOS expression, and in turn has prominent functional effects in sinusoidal endothelial cells. Overexpression of ILK increased eNOS expression, and as a result, eNOS phosphorylation. Additionally, inhibition of ILK activity with QLT-0267 or its knockdown induced a reduction in eNOS promoter activity (**Figure 5**) resulting in decreased eNOS expression and subsequent eNOS phosphorylation. We have also shown that ILK expression was significantly upregulated in sinusoidal endothelial cells after liver injury, by cytokines and/or peptides typical of the injury environment.

The role of ILK in vascular endothelial cells has been the topic active investigation. Lack of ILK specifically in endothelial cells leads to endothelial cell detachment, loss of actin fibers and defective vascular development (20). ILK appears to also be important in survival, function of endothelial cells (21) and cell adhesion, suggesting a role for ILK in EC-ECM interaction and endothelial function (22). Another important function of endothelial cells is NO production via eNOS. One study demonstrated that NO production was enhanced by overexpression of ILK (14). In this study, we have extended these data to indicate that ILK is important in eNOS biology in specialized endothelium – hepatic sinusoidal endothelial cells. Further, since eNOS is critical in sinusoidal endothelial function, including in the pathogenesis of portal hypertension, we speculate that ILK may likewise play a role in the pathogenesis of portal hypertension.

Abundant evidence indicates that injury to the liver is associated with an endothelialopathy, with resultant impaired NO release by the endothelium (3, 23). We and others have demonstrated that eNOS phosphorylation in sinusoidal endothelial cells is abnormal after injury, likely due to abnormal post-translational modification(s) (**Figure 8**); for example, Akt phosphorylation and subsequent activation of eNOS enzymatic activity are reduced in injured compared to normal sinusoidal endothelial cells (16, 24). These data, together with those from the current study raise questions about the role of ILK in regulation of eNOS derived NO. For example, injury and/or various cytokines/peptides led to increased ILK expression, which in turn led to increased P-eNOS expression and NO production in isolated cells. Given that in the injured liver, NO production is reduced, the implication is that there must be other factors that mitigate the effect of apparent stimulatory effect of ILK.

One such player is Rho, important in the cytoskeleton/ILK axis, which appeared to have prominent effects on eNOS expression. We showed that Rho activation led to a decrease in eNOS mRNA and protein expression, while Rho inhibition had the opposite effect. Additionally, inhibition of Rho-GTPase caused a significant increase in eNOS phosphorylation. Thus, to the extent that the Rho and ILK pathways interact, this axis is likely to be important in modulation of ILKs effects and like ILK, may be important in vascular disorders.

The mechanism underlying the effect of ILK on eNOS expression is unknown. It is attractive to speculate that the actin cytoskeleton may play a role. For example, we found that inhibition of ILK markedly disrupted the actin cytoskeleton (**Figure 4**), raising a possible link between the cytoskeleton and eNOS expression/function. However, it should be emphasized that additional pathways are likely involved. For example, we have shown previously that G-protein-coupled receptor kinase-2 (GRK2) expression is increased in injured sinusoidal endothelial cells from portal hypertensive rats. Akt physically interacts with G-protein-coupled receptor kinase-2 (GRK2), and that this interaction inhibits Akt phosphorylation and NO production (5). Therefore, while the GRK2/Akt pathway does not appear to affect eNOS protein expression, it clearly plays a role in eNOS phosphorylation and signaling, and it is possible that Rho and/or ILK intersects with the Akt/GRK2 pathway, further modifying eNOS function.

In summary, we have shown that ILK has critical effects on eNOS in sinusoidal endothelial cells. Further, we have reported that the Rho signaling pathway is important in phosphorylation of Akt and eNOS expression and activity. Because activation of eNOS is fundamental to the maintenance of normal vascular function, and Rho seems to play an important role in vascular diseases, these data suggest that inhibition of Rho might exert beneficial effects in portal hypertension.

Acknowledgments

This work was supported by the NIH (Grant R01 DK 57830 to DCR). We thank Dr. Yoon Jun Kim (Seoul National University Hospital) for discussion about this topic and performance of preliminary experiments that led to creation of the final body of work.

Abbreviations

SECs	sinusoidal endothelial cell
eNOS	endothelial nitric oxide synthase
ILK	integrin-linked kinase
NO	nitric oxide
ET-1	endothelin-1
CCl_4	carbon tetrachloride
BDL	bile duct ligation
Ad-GFP	adenovirus GFP
EGF	epidermal growth factor
VEGF	vascular endothelial growth factor
TGF-β	transforming growth factor beta1
DMSO	dimethyl sulfoxide

References

1. LOPEZ-RIVERA E, LIZARBE TR, MARTINEZ-MORENO M, et al. Matrix metalloproteinase 13 mediates nitric oxide activation of endothelial cell migration. Proc Natl Acad Sci U S A. 2005; 102(10):3685–90. [PubMed: 15728377]
2. TSAO PS, COOKE JP. Endothelial alterations in hypercholesterolemia: more than simply vasodilator dysfunction. J Cardiovasc Pharmacol. 1998; 32(Suppl 3):S48–53. [PubMed: 9883748]
3. ROCKEY DC, CHUNG JJ. Reduced nitric oxide production by endothelial cells in cirrhotic rat liver: endothelial dysfunction in portal hypertension. Gastroenterology. 1998; 114(2):344–51. [PubMed: 9453496]
4. YU Q, SHAO R, QIAN HS, GEORGE SE, ROCKEY DC. Gene transfer of the neuronal NO synthase isoform to cirrhotic rat liver ameliorates portal hypertension. J Clin Invest. 2000; 105(6): 741–8. [PubMed: 10727442]
5. LIU S, PREMONT RT, KONTOS CD, ZHU S, ROCKEY DC. A crucial role for GRK2 in regulation of endothelial cell nitric oxide synthase function in portal hypertension. Nat Med. 2005; 11(9):952–8. [PubMed: 16142243]

6. GARCIA-CARDENA G, FAN R, STERN DF, LIU J, SESSA WC. Endothelial nitric oxide synthase is regulated by tyrosine phosphorylation and interacts with caveolin-1. J Biol Chem. 1996; 271(44):27237–40. [PubMed: 8910295]
7. FULTON D, GRATTON JP, MCCABE TJ, et al. Regulation of endothelium-derived nitric oxide production by the protein kinase Akt. Nature. 1999; 399(6736):597–601. [PubMed: 10376602]
8. LIU S, PREMONT RT, ROCKEY DC. G-protein-coupled receptor kinase interactor-1 (GIT-1) is a new endothelial nitric oxide synthase (eNOS) interactor with functional effects on vascular homeostasis. J Biol Chem. 2012 Epub ahead of print.
9. HALL A. Rho GTPases and the actin cytoskeleton. Science. 1998; 279(5350):509–14. [PubMed: 9438836]
10. LAUFS U, LIAO JK. Targeting Rho in cardiovascular disease. Circ Res. 2000; 87(7):526–8. [PubMed: 11009552]
11. LAUFS U, LIAO JK. Post-transcriptional regulation of endothelial nitric oxide synthase mRNA stability by Rho GTPase. J Biol Chem. 1998; 273(37):24266–71. [PubMed: 9727051]
12. LAUFS U, ENDRES M, STAGLIANO N, et al. Neuroprotection mediated by changes in the endothelial actin cytoskeleton. J Clin Invest. 2000; 106(1):15–24. [PubMed: 10880044]
13. CHISWELL BP, ZHANG R, MURPHY JW, BOGGON TJ, CALDERWOOD DA. The structural basis of integrin-linked kinase-PINCH interactions. Proc Natl Acad Sci U S A. 2008; 105(52): 20677–82. [PubMed: 19074270]
14. GONZALEZ-SANTIAGO L, LOPEZ-ONGIL S, RODRIGUEZ-PUYOL M, RODRIGUEZ-PUYOL D. Decreased nitric oxide synthesis in human endothelial cells cultured on type I collagen. Circ Res. 2002; 90(5):539–45. [PubMed: 11909817]
15. PROCTOR E, CHATAMRA K. High yield micronodular cirrhosis in the rat. Gastroenterology. 1982; 83(6):1183–90. [PubMed: 7129027]
16. LIU S, PREMONT RT, KONTOS CD, HUANG J, ROCKEY DC. Endothelin-1 activates endothelial cell nitric-oxide synthase via heterotrimeric G-protein betagamma subunit signaling to protein jinase B/Akt. J Biol Chem. 2003; 278(50):49929–35. [PubMed: 14523027]
17. SHAFIEI MS, ROCKEY DC. The role of integrin-linked kinase in liver wound healing. J Biol Chem. 2006; 281(34):24863–72. [PubMed: 16728409]
18. LAUFS U, ENDRES M, CUSTODIS F, et al. Suppression of endothelial nitric oxide production after withdrawal of statin treatment is mediated by negative feedback regulation of rho GTPase gene transcription. Circulation. 2000; 102(25):3104–10. [PubMed: 11120702]
19. SHAFIEI MS, ROCKEY DC. The function of integrin-linked kinase in normal and activated stellate cells: implications for fibrogenesis in wound healing. Lab Invest. 2012; 92(2):305–16. [PubMed: 22064318]
20. SAKAI T, LI S, DOCHEVA D, et al. Integrin-linked kinase (ILK) is required for polarizing the epiblast, cell adhesion, and controlling actin accumulation. Genes & development. 2003; 17(7): 926–40. [PubMed: 12670870]
21. CHO HJ, YOUN SW, CHEON SI, et al. Regulation of endothelial cell and endothelial progenitor cell survival and vasculogenesis by integrin-linked kinase. Arteriosclerosis, thrombosis, and vascular biology. 2005; 25(6):1154–60.
22. WU C, DEDHAR S. Integrin-linked kinase (ILK) and its interactors: a new paradigm for the coupling of extracellular matrix to actin cytoskeleton and signaling complexes. The Journal of cell biology. 2001; 155(4):505–10. [PubMed: 11696562]
23. ROCKEY DC. Vascular mediators in the injured liver. Hepatology. 2003; 37(1):4–12. [PubMed: 12500181]
24. FERNANDEZ-VARO G, MELGAR-LESMES P, CASALS G, et al. Inactivation of extrahepatic vascular Akt improves systemic hemodynamics and sodium excretion in cirrhotic rats. J Hepatol. 2010; 53(6):1041–8. [PubMed: 20800923]

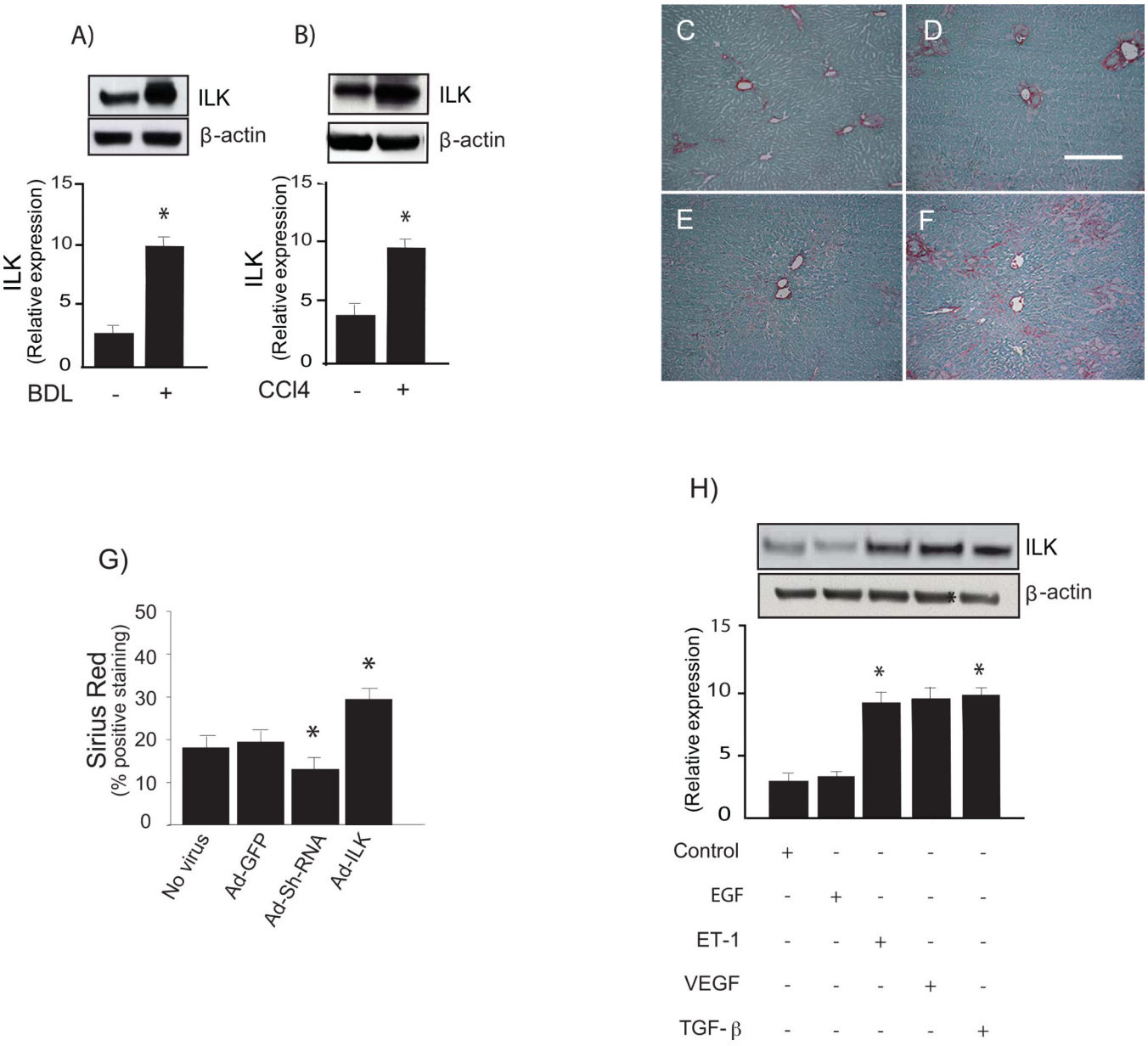

Figure 1. Increased expression of ILK after liver injury

In (A-B), liver injury was induced by bile duct ligation and CCl_4 as described in "Experimental procedures" and sinusoidal endothelial cells were isolated and allowed to adhere for 18 hours on collagen-coated culture plates. Cells were harvested and lysates (50 μg total protein) were subjected to immunoblotting with specific antibody directed against ILK or μ-actin. Below the representative, respective immunoblots, data were quantified, normalized to the signal for μ-actin, and presented graphically (*n*-5, *`*p* < 0.05 vs. normal animals). In (C-G), bile duct ligation was performed as in "Experimental Procedures." During surgery, an adenovirus containing GFP (Ad-GFP), ILK (Ad-ILK), or shILK (Ad-shILK) were injected, also as in "Experimental Procedures" in to the inferior vena cava (concentration of 10^{10}/plaque-forming units/kg in 500 μl of PBS). Ten days later, livers were harvested and subjected to picrosirius red staining as described under "Experimental

Procedures." Representative liver sections are shown from rats undergoing sham BDL + Ad-GFP (C), BDL + Ad-GFP (D), or those additionally exposed to Ad-ShILK (E) or Ad-ILK (F). The scale bar shown represents 50 microns. Histomorphometric analysis was performed on random picrosirius red-stained liver sections (G). In (H), sinusoidal endothelial cells were serum-starved for 18 hours and exposed to EGF (10μg/ml), ET-1 (10 nM) VEGF (30 ng/ml) TGF-β (10 ng/mL) for 24 hours and subjected to immunoblotting for ILK detection. A representative ILK immunoblot is shown in the upper panel, and below it, a stripped blot re-probed for μ-actin; below the immunoblots, data from independent experiments were quantified, normalized to the signal for β-actin and presented graphically (n =3; *p <0.05 vs. control).

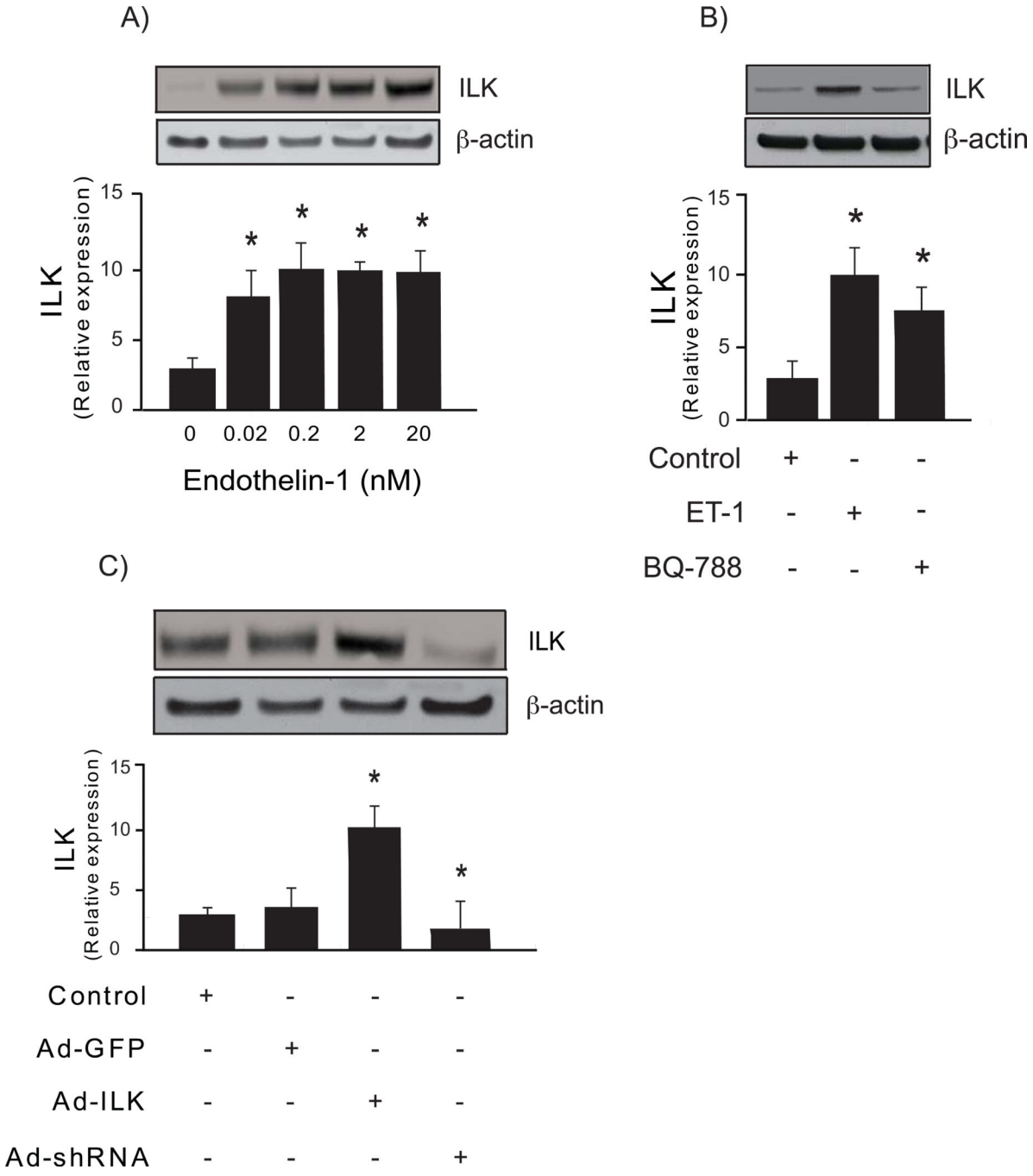

Figure 2. Regulation of ILK expression

In (A), sinusoidal endothelial cells were isolated and then serum-starved and exposed to ET-1 at the indicated concentrations for 24 hours and subjected to immunoblotting to detect ILK (50 μg total protein from the cell lysate). A representative immunoblot is shown in the upper panel, and below it, a stripped blot re-probed to detect β-actin; below the immunoblots, data from independent experiments were quantified, normalized to the signal for β-actin and presented graphically (n =3; *p <0.05 vs. control (no endothelin-1)). In (B), sinusoidal endothelial cells were as in (A), and were subsequently exposed to 20 nM ET-1

for 24 hours in the absence or presence of BQ-788 (20 nM, an endothelin-B receptor antagonist). In the upper panel of (B), representative immunoblots as in (A) are shown (ILK, top panel, and β-actin, lower panel), and in the bottom panel, data were quantified, normalized to the signal for β-actin, and presented graphically (n =3; *p <0.05 vs. control). In (C), sinusoidal endothelial cells were transduced with the indicated recombinant adenoviruses (Ad-ILK-expressing ILK, Ad-shILK-expressing small interfering short hairpin ILK RNA, or adenovirus containing the identical adenovirus backbone without a cDNA insert Ad-GFP) as described in “Experimental Procedures”, each at a multiplicity of infection of 100. Cell lysates (50 μg total protein) were subjected to immunoblotting with anti-ILK antibody as described in “Experimental Procedures”. Representative immunoblots are shown in the top panel of the figure, and in the bottom panel of the figure, data from independent experiments were quantified, normalized, and presented graphically (n=3; *p <0.01 vs. Ad-GFP).

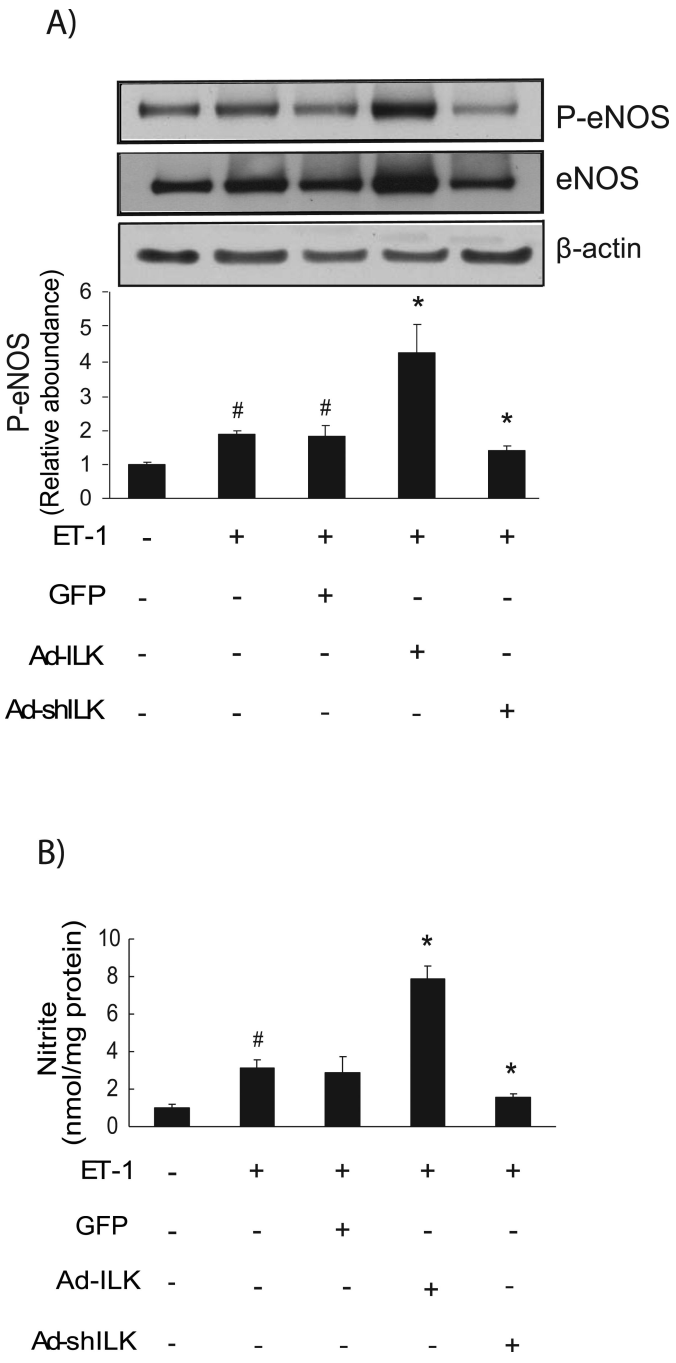

Figure 3. ILK regulates P-eNOS and NO production

In (A), sinusoidal endothelial cells were infected with the indicated recombinant adenoviruses (Ad-ILK, Ad-shILK, or Ad-GFP), each at a multiplicity of infection of 100. Cells were washed and incubated in serum-free medium for 6 h, followed by exposure to ET-1 (10 nM) for 30 min. Cellular lysates (50 μg total protein) were subjected to immunoblotting with anti P-eNOS after which blots were stripped and reprobed with anti-total eNOS antibody and anti-β actin antibody. The data shown are representative of three different experiments, each performed with cells from a different isolation (n =3; *p < 0.05

vs. control; # $p < 0.01$ vs. Ad-ILK). Representative immunoblots are shown in the top panel of the figure, and in the bottom panel of the figure. In (B), conditioned medium from the same cells was collected, and nitrite levels were measured by chemiluminescence as in "Experimental Procedures" ($n = 3$; *$p < 0.005$ *versus* control; # $p < 0.01$ *versus* Ad-ILK).

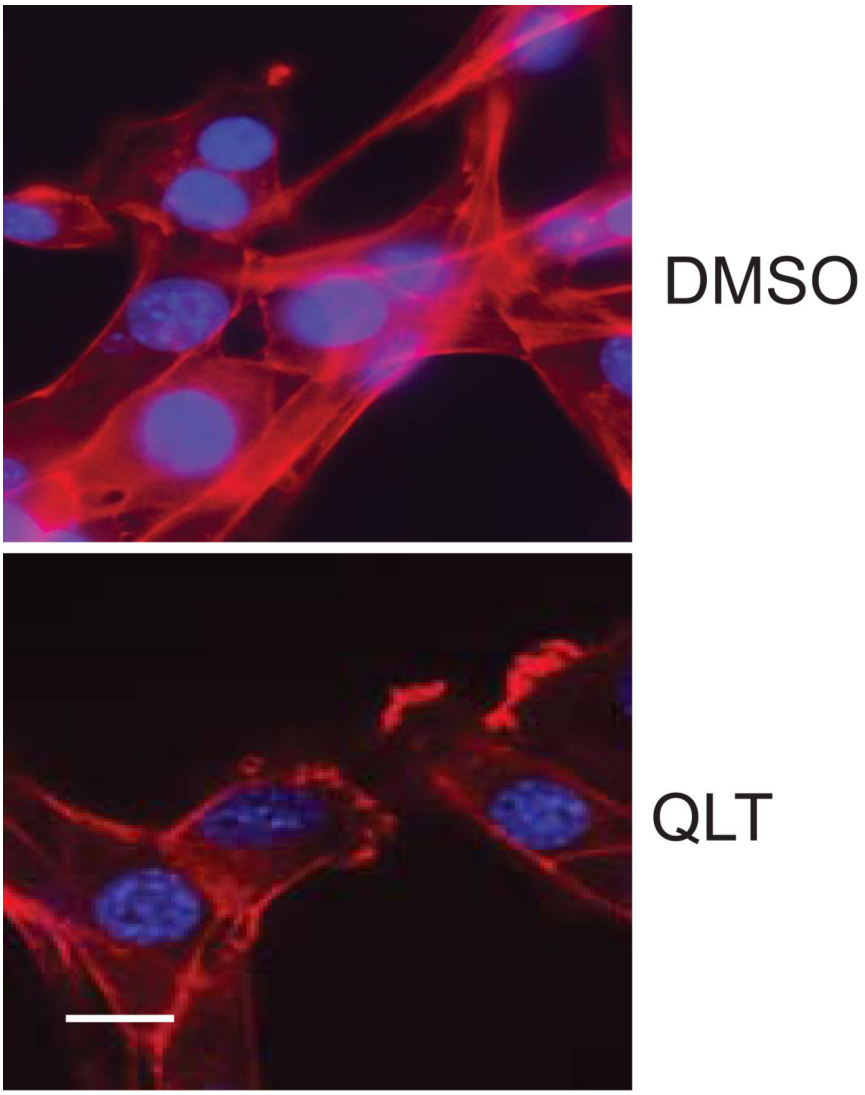

Figure 4. ILK inhibition disrupts the actin cytoskeleton

Sinusoidal endothelial cells were isolated from rat livers and exposed to 25μM QLT-0267 for 36h (bottom panel), DMSO was used as a control (top panel) since this is what QLT-0267 was mixed in prior to addition to medium. Cells were fixed and labeled with rhodamine-phalloidin (red) and DAPI (blue) as in Methods. Representative (of > 10 other examples) images are shown. The scale bar represents 5 microns.

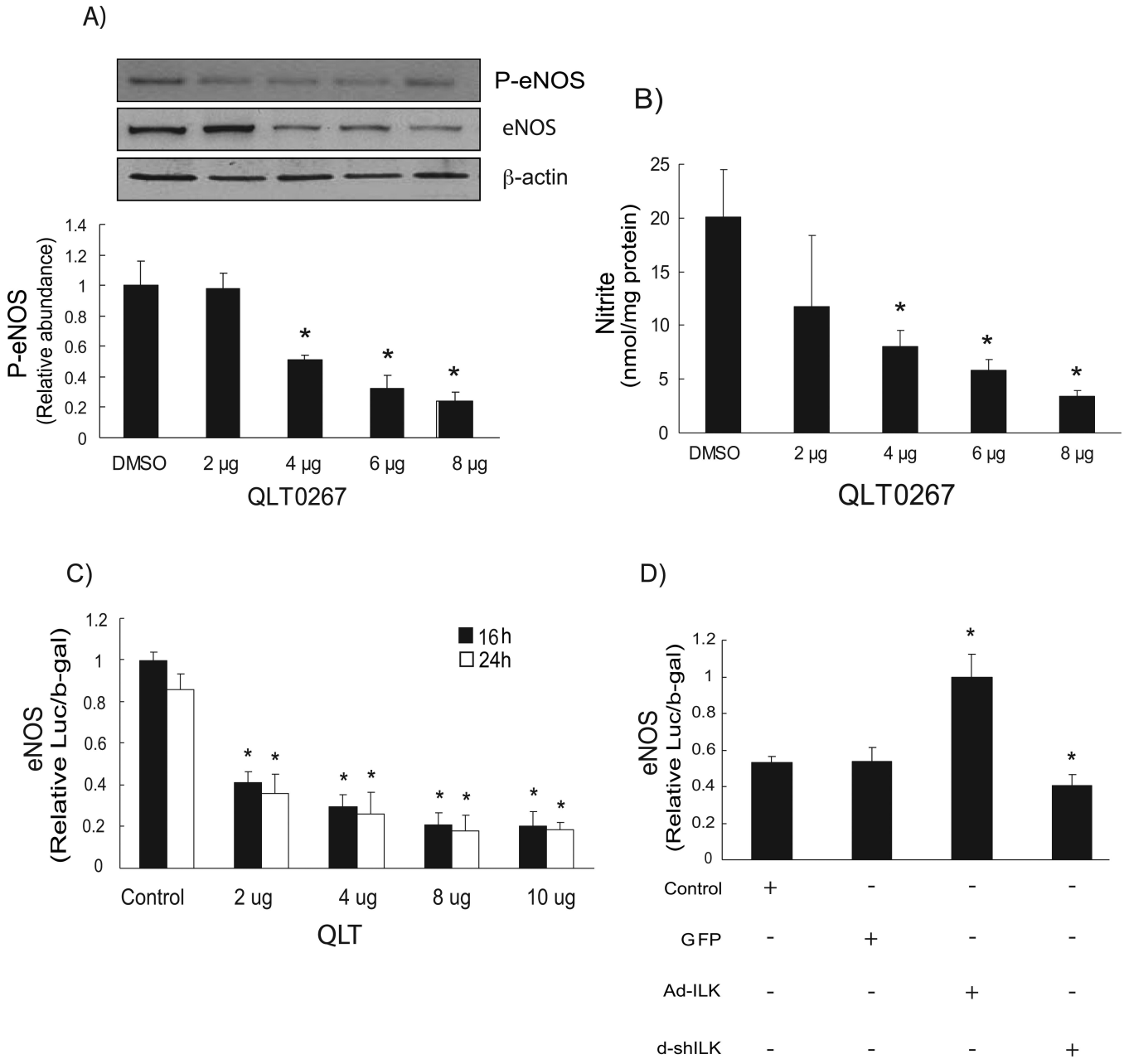

Figure 5. ILK kinase inhibition negatively regulates P-eNOS and NO production

In (A), sinusoidal endothelial cells were serum-starved and exposed to QLT-0267 at the indicated concentration (μg/mL). Cells were harvested and lysates (50 μg total protein) were subjected to immunoblotting with specific antibody directed against P-eNOS. Below the representative, respective immunoblot, data were quantified, normalized to the signal for eNOS and β-actin, and presented graphically (n=5; *p < 0.05 vs. DMSO control). The immunoblots shown are representative of three different experiments, each performed with cells from a different isolation. In (B), NO production in the same sinusoidal endothelial cells was detected by chemiluminescence detection of nitrites in conditioned medium as described in “Experimental Procedures” (n =3; *, p <0.005 vs. DMSO control). In (C),

sinusoidal endothelial cells were serum-starved and exposed to QLT-0267 as in (A), and luciferase activity was assayed as described in “Experimental Procedures” ($n = 3$; $^*P < 0.05$ vs. corresponding control). In (D), sinusoidal endothelial cells were infected with the indicated adenoviruses (Ad-ILK, Ad-shILK or Ad-GFP) as described under “Experimental Procedures,” each at a multiplicity of infection of 100 for 24 hours and luciferase activity was assayed as in C ($n = 3$; $^*p < 0.05$ vs. corresponding control).

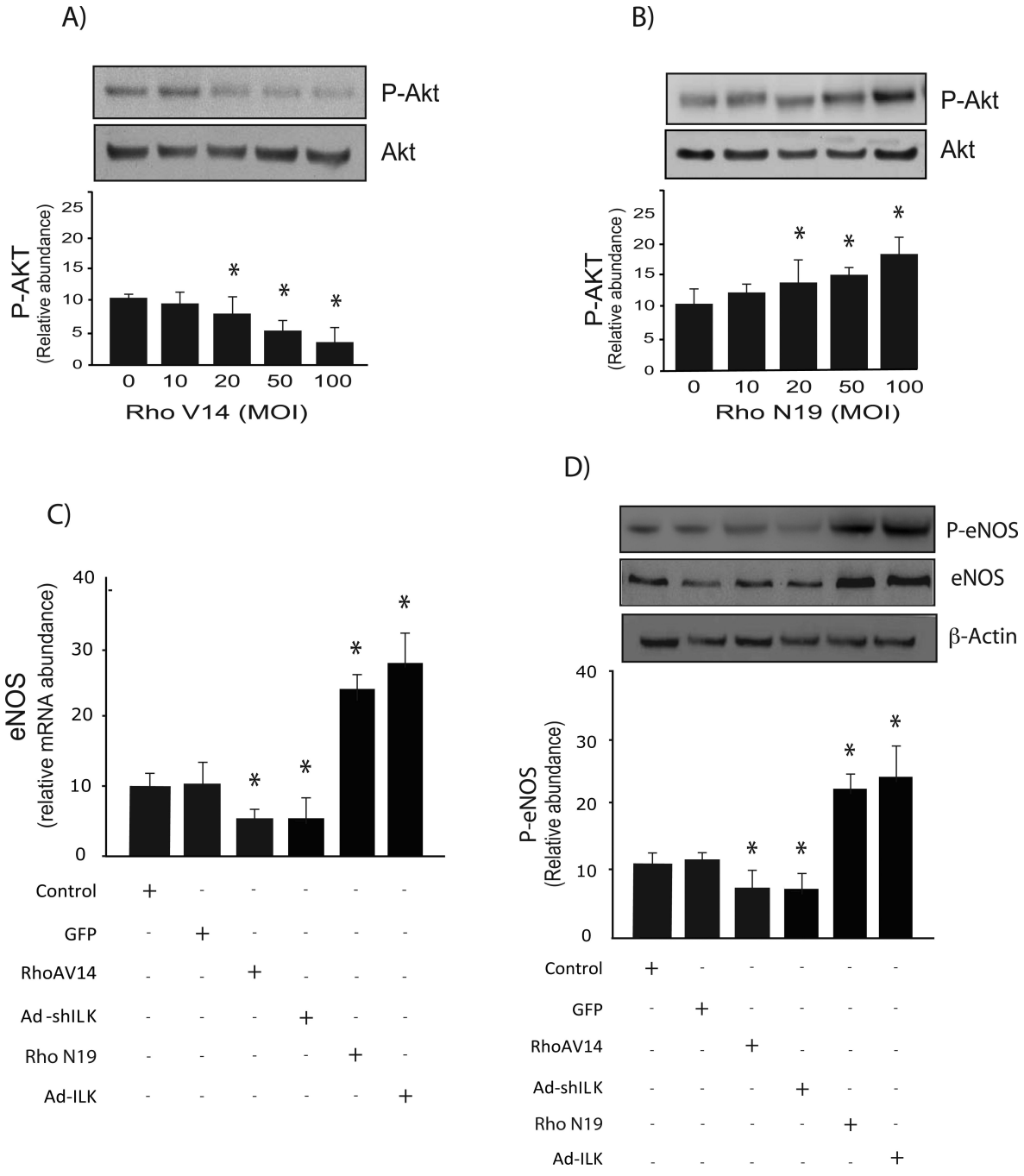

Figure 6. Rho differentially modulates Akt and eNOS phosphorylation

In (A & B), sinusoidal endothelial cells were infected with the indicated recombinant adenoviruses, respectively at a multiplicity of infection of 100 for 24 hours as in "Experimental Procedures". Cell lysates (50 μg total protein) were subjected to immunoblotting with anti P-Akt antibody as described in "Experimental Procedures". Below the representative, respective immunoblot, data were quantified, normalized to the signal for Akt, and presented graphically (n=5, *p < 0.05 vs. control). In (C), sinusoidal endothelial cells were infected with the indicated adenoviruses, each at a multiplicity of infection of 100

for 24 hours as in A &B, and mRNA levels were measured by RT-PCR as described as in "Experimental Procedures", and the data presented graphically (n=3, * $p < 0.05$, vs. control). In (D), cells were as in (C), and cell lysates (50 μg total protein) were subjected to immunoblotting with the indicated antibodies (including a stripped blot reprobed for eNOS and β-actin); representative immunoblots are shown in the upper panel, and below it, data from independent experiments were quantified, normalized and presented graphically (n =3, *$p < 0.05$ vs. control).

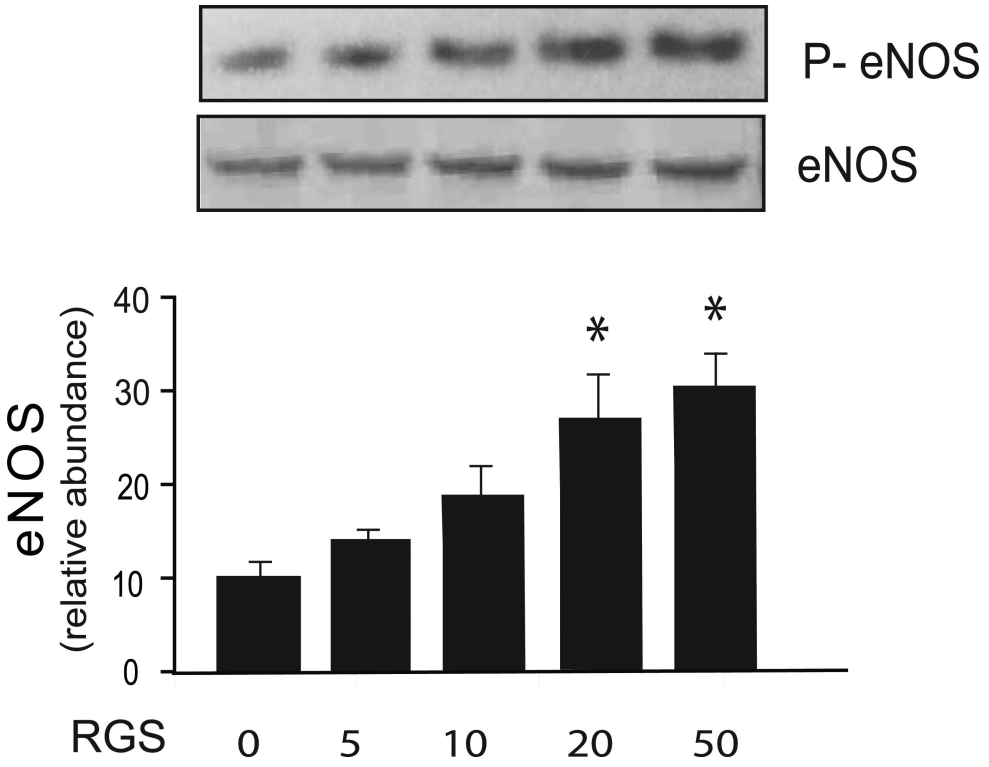

Figure 7. Rho inhibition inhibits eNOS function

Sinusoidal endothelial cells were isolated and infected with recombinant RGS adenovirus at the indicated multiplicity of infection for 24 hours as in "Experimental Procedures". Cell lysates (50 μg total protein) were subjected to immunoblotting with anti-phospho-eNOS antibody and a stripped blot re-probed for eNOS subsequently. Representative immunoblots are shown in the upper panel, and below it data from independent experiments were quantified, normalized and data presented graphically (n =3, *p <0.05 vs. control).

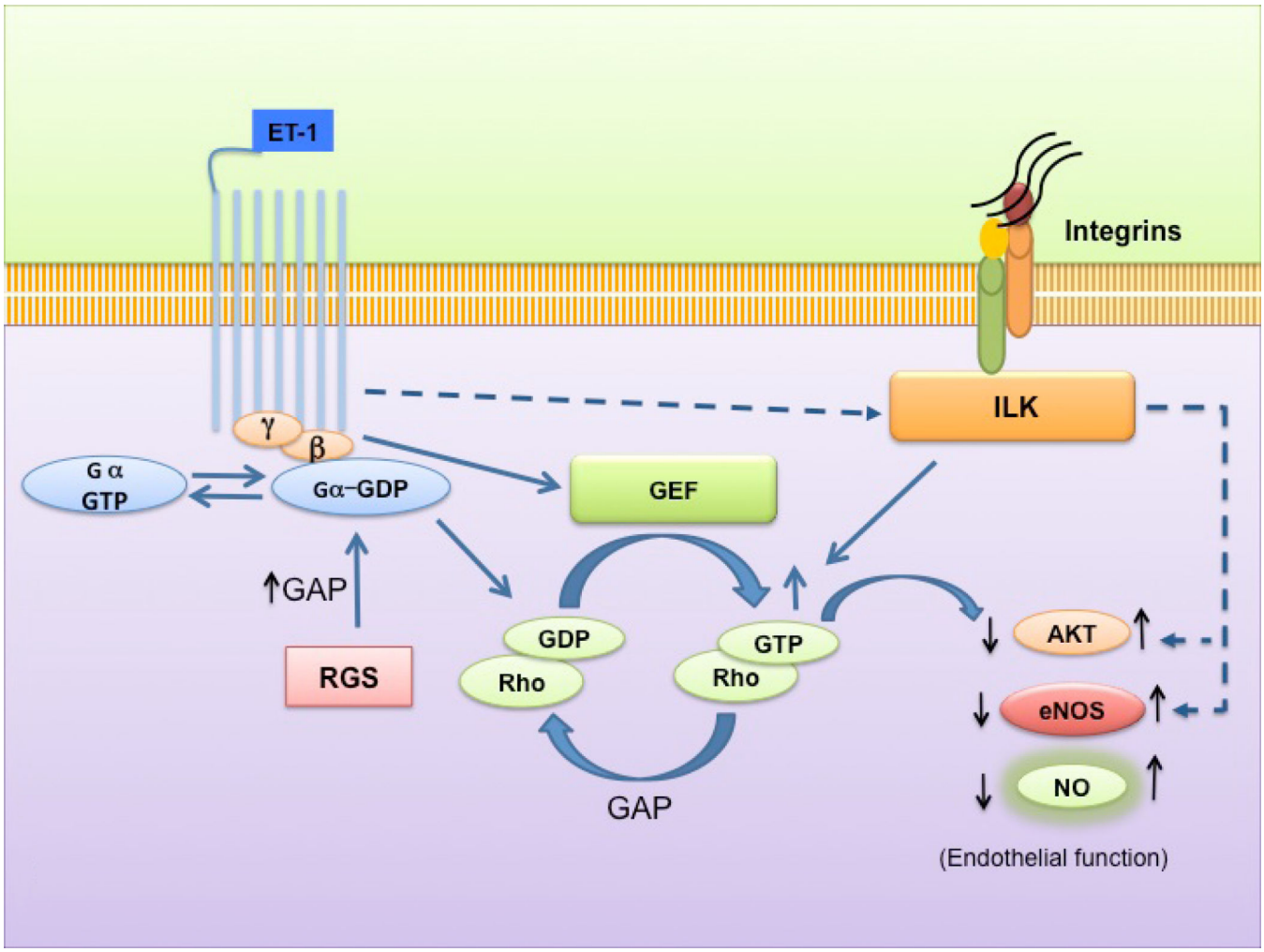

Figure 8. A working model for integrin linked kinase (ILK), Rho, and eNOS in sinusoidal endothelial cells

The figure highlights previously established ILK signaling patterns and emphasizes data from the current study. Specific mediators such as endothelin-1 (ET-1) and/or liver injury stimulate ILK expression. ET-1 and injury induced changes in ILK expression lead to upregulation of in Akt and eNOS signaling, and ultimately increased NO production. eNOS expression is also downregulated by Rho, leading to an effect that is opposite of ILK, which ultimately leads to reduced NO production.